2012

Microlens array light trapping in CdTe/CdS solar cells

Patrick Michael Margavio

Department:

MICROLENS ARRAY LIGHT TRAPPING IN CdTe/CdS SOLAR CELLS

By

PATRICK MARGAVIO

A THESIS

Presented to the Faculty of the Graduate School of the

MISSOURI UNIVERSITY OF SCIENCE AND TECHNOLOGY

In Partial Fulfillment of the Requirements for the Degree

MASTERS OF SCIENCE IN MECHANICAL ENGINEERING

Approved by

Hai-Lung Tsai, Co-advisor
Hai Xiao, Co-advisor
Kelly Homan

ABSTRACT

In light of the continued rise in fossil fuel costs, alternative energy sources, such as solar technology, are increasingly important. Concentrating photovoltaic systems are promising for future efficient and cost effective competition with fossil fuels. A microlens array is employed to a CdTe/CdS semiconducting solar cell to increase efficiency via light trapping. Since the microlens array will cause a local increase in incident light intensity, it should cause a corresponding increase in efficiency. The solar cell is deposited layer by layer. The CdS layer is chemically deposited. The CdTe layer is deposited using a novel additive manufacture technique: laser melting of CdTe powder. A $CdCl_2$ thermal treatment is implemented following CdTe deposition to compensate for CdTe/CdS lattice mismatch. A microlens array mold is etched out of foturan glass that has been treated with femtosecond laser exposure. PDMS (polydimethylsiloxane) microlens arrays are cast from this foturan glass mold to greatly decrease manufacture costs of the microlens array. The use of a glass mold for PDMS casting improves lifetime of mold as compared to conventional approaches. The efficiency without the microlens array is 2.19% and it is 2.26% with the microlens array. Reliability difficulties were observed in electrical characterization as well as a low overall efficiency. It is theorized that these difficulties were caused by the laser melting technique used to fabricate the CdTe layer.

ACKNOWLEDGEMENTS

The author is grateful to the Intelligent Systems Center at Missouri University of Science and Technology for financial support of this project. He would like to thank his coworker Dr. Cheng-Hsiang Lin for assistance with the microlens array mold processing. He would also like to thank Dr. Leedy of Wright-Patterson Air Force Base for sputtering of back contact. He would also like to thank the graduate thesis defense committee members: Dr Hai-Lung Tsai, Dr Hai Xiao, and Dr Kelly Homan.

TABLE OF CONTENTS

LIST OF FIGURES

LIST OF TABLES

1. INTRODUCTION

1. 1. PHOTOVOLTAICS

The need for solar energy has come to the forefront of public attention in recent years as an effort has been made to begin replacing fossil fuels with renewable energy sources. The United Nations Framework Convention on Climate Change calls for 10TW of carbon-emission-free power to be produced by the year 2050, almost equivalent to the power provided by all of today's energy sources combined[1]. Solar energy is an attractive alternative to fossil fuels due to the large amount of energy provided to the earth by the sun (120,000TW of energy reaches the earth from the sun[1]). The challenge is to make solar cost-competitive with the currently available fossil fuels. One of the promising technologies in the solar energy field is photovoltaics (PV). Photovoltaic cells convert solar radiation directly into electricity in a variety of different ways.

Solar thermal technologies have been much more prevalent in engineering applications than have photovoltaics. When comparing different technologies via end use matching, it becomes obvious, for example, that solar thermal techniques are well suited to provide domestic hot water for residential applications (among other things). It turns out that PV technologies have a niche all their own. Amongst photovoltaic technologies there are crystalline PV (also known as bulk PV), such as polycrystalline silicon, and there are thin film technologies. Crystalline technologies are currently those being explored for large scale power generation. The CdTe/CdS solar cell used in this project is a thin film technology. The benefit of thin film technologies over crystalline

technologies (and solar thermal) are primarily that of flexibility; thin film solar cell technologies have many potential applications that are not available to other kinds of solar cell technologies. For example, thin film solar cells could be built on flexible polymer substrates and installed on a variety of materials. They could be embedded in fabric. They could be added inside of window panes (or blinds) to generate electricity while they provide desired shade for occupants of the building. Due to this increased flexibility in applications, thin film technologies are promising future technology for many engineering applications.

When considering PV, there are two basic approaches which have been used to attempt to achieve cost-competition with fossil fuels. The first approach is to make PV as inexpensive as possible (i.e. relatively low efficiency cells which are very cheap). This approach has been employed in single-crystal and polycrystalline silicon, Copper Indium Gallium Diselenide, Dye Sensitized solar cells, and other technologies. The second approach is to create a highly efficient solar cell (i.e. a cell that is relatively more expensive, but makes effective use of most of the energy it receives from the sun). The second approach is what inspired the creation of multijunction solar cells and other high efficiency high cost solar technologies. As an illustration, GaAs multijunction solar cells have reached the highest recorded efficiency for solar cells yet, 42.3%[2]. Triple junction silicon has also demonstrated high efficiency[3]. The problem with using high efficiency cells is that they are too expensive, in their own right, to be cost competitive with fossil fuels. That is where solar concentration comes into play. In many cases, depending on the intended application, the choice between a non-concentrating technology (low cost,

low efficiency) and a concentrating technology (high efficiency combined with concentrator) may be simply an engineering design choice.

1.2. SOLAR CONCENTRATION

Solar energy concentration is any technique which increases the intensity of incident light on the solar cell above that of ambient solar radiation. Examples of solar concentrator technologies include Luminescent solar concentrators, large parabolic mirrors, etc. Concentrating solar energy adds little in the way of expense to the solar power system. In typical solar concentrator systems, the solar cell itself comprises an average of about 75% of the cost of the system. Solar cells are more efficient in approximate proportion to the intensity of light incident on their surface. Thus, increasing that intensity, via concentration, increases the efficiency. By combining solar concentration techniques with high efficiency solar cells, cost competitive PV systems become possible.

Another popular technique to increase efficiency is to implement a light trapping mechanism. Generally, any technique that causes light to remain inside a solar cell for a longer period of time is a light trapping technique (light trapping is sometimes considered a subset of, or equivalent to, solar concentration). Many ideas have been implemented to trap solar energy in a cell, including anti-reflective coatings, changing surface geometry to scatter light internally, back scattering light off the back contact, and many approaches which involve nanostructures.

1.3. MICROLENS ARRAYS

The goal of this research is to determine if a microlens array can be used as an effective solar concentrator technique and thereby generate higher system efficiencies. A microlens array is an orderly assembly of microscopic lenses. The creation of a microlens array can be very costly. A novel approach is presented to make microlens arrays affordable. The current technique is to use a metallic mold for the silicon (PDMS or otherwise) lens array casting. The casting process is corrosive to the metallic molds. Thus these expensive molds must be replaced frequently. Using a glass mold that has been fabricated by laser direct writing produces a longer lasting mold for silicon casting. Cylindrical microlens array molds embedded in photosensitive Foturan glass were fabricated by femtosecond (fs) laser micromachining. This glass mold can then be used as a template for creation of silicon (Polydimethylsiloxane (PDMS)) microlens arrays. The time commitment and cost of producing PDMS arrays is very small. The primary cost in the process is in the production of the photosensitive glass mold. As an illustration of the time saved in using a PDMS lens rather than a glass lens, consider the time to manufacture one hundred 1 square foot arrays. Using the laser to create those lenses in glass would take 1,379 years. Using the laser mold with PDMS lenses would take only 300 days. Without PDMS it is not doable. In this example, I am assuming the use of only one laser to manufacture lenses; it would be possible to further increase the speed of production, to only 2 days, by splitting the laser beam and simultaneously fabricating multiple molds. More time is saved the larger the area of manufacture, so it scales well to industrial scales.

The dimensions of the microlens array were chosen carefully. They are detailed in Figure 1-1. Five hundred microns is added to the bottom of the lenses to add mechanical strength to the PDMS lens array.

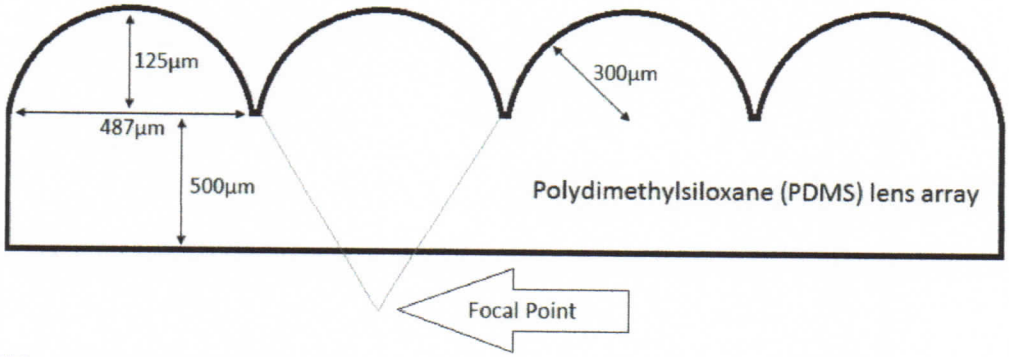

Figure 1-1. Schematic of Lens Array Dimensions.

The focal length is 50 microns below the bottom of the lens array so that light will be focused inside the solar cell. The Lensmaker's Equation for a Plano-Convex lens relates the focal length (f) to the radius of curvature (R) for this lens design:

$$\frac{1}{f} = \frac{n-1}{R}$$

where the index of refraction of float glass (1.48) is denoted as n. Using this relationship, the dimensions necessary to produce a focal length 50 microns below a 500 micron layer can be easily calculated. There are many other possible applications for microlens arrays, some of these applications require smaller lenses to be fabricated. My technique of microlens array fabrication can be easily applied to fabricate lenses that are smaller[4].

1.4. CdTe/CdS SOLAR CELL

In order to test the application of a microlens array as a solar concentrator technique, a solar cell design was chosen. The design chosen for this test was a CdS/CdTe solar cell. CdTe is used widely in thin film solar cell applications due to the fact that it is a direct bandgap material with an energy gap of 1.45eV and an absorption coefficient of 10^5/cm in the visible region. This means that a layer thickness of a few micrometers is sufficient to absorb ~90% of the incident photons[5]. This is highly significant since 43% of the irradiance from the sun is in the visible spectrum[6]. The visible part of the solar spectrum contains the largest amount of energy since infrared light is relatively low energy (due to its longer wavelength) and the UV part of the spectrum composes relatively low intensity and is blocked heavily by the upper atmosphere. Thus, most of the energy that reaches the earth from the sun is in the visible part of the spectrum. Since CdTe is an excellent absorber in the visible spectrum, it is an ideal material for high-efficiency, low-cost thin film solar cells. Additionally, CdTe semiconducting PV cells have reached efficiencies as high as 16.5%[7]. These efficiencies are among the highest efficiencies currently achievable in thin film solar cells (the highest being Cu(In, Ga)Se_2 with 17.1%[8]). Ideally, a microlens array would be applied to

a high efficiency PV technology like multi-junction GaAs in concert with another solar concentrating technique to provide maximum increase in efficiency, but CdTe/CdS will experimentally suffice to demonstrate the effect of microlens arrays on solar technology.

2. EXPERIMENTATION

2.1. PHOTOSENSITIVE GLASS MOLD FABRICATION

The fs laser system used in the experiment is a regeneratively amplified Ti:sapphire laser (Legend-F, Coherent) whose repetition rate, center wavelength, and pulse duration are 1kHz, 800nm, and 120fs, respectively. The maximum output power of the fs laser is 1 W, which corresponds to a pulse energy of 1mJ. The laser beam was attenuated to 0.72% of its maximum intensity and then focused through a microscope objective lens onto the glass sample. The fact that the intensity required for mold fabrication is so small implies that it will scale well to industrial applications; that is because the laser beam may be split into many beams that are each 0.72% of the maximum intensity and produce many molds at once. The Foturan glass sample was mounted on a five axis motion stage (Aerotech) with a resolution of 1μm. Before the program was executed to move the motion stage, half an hour was allowed for the laser system to stabilize. Then, the motion stage was instructed to move in an arc of period 487μm with radius of curvature 300μm in the x-z plane. This motion was repeated as the motion stage moved in the y direction in increments of 1 micrometer. This is performed until the laser has traveled 2mm in the y direction. After this is achieved, the code moves to the endpoint of this first trough to start the process of creating a second trough. The two troughs will create one lens of length 4mm. After this second run is complete, the code moves back to the start position and then over in the x direction by 0.487mm so that a second lens can be made next to the first. This is repeated until 4 lenses are created of length 4mm each. At each step in the process, the pattern is repeated 8 times at higher

and higher locations in the z direction. The increment of motion in the z direction is 15μm. These repetitions at successively higher z values are performed so that all the Foturan glass inside the cylinder lens shape will be exposed. A complete description of this procedure can be found in the literature[4]. The total time to complete the lens array mold is approximately 90 hours. Due to the fact that our laser could operate continuously for only 16 hours, the mold fabrication had to broken up over several days. This is why the lenses were created in 2mm length pieces. Each day one eight of the lens mold was fabricated (~11 hours) and the laser system was stopped to allow for six to eight hours of cool down time. Repeating this process, the mold was fabricated over the course of 8 days.

After the laser processing of the Foturan glass, a postprocessing procedure is required. The Foturan glass must be thermally treated in a programmable furnace (Fischer Scientific) to develop the modified region inside the glass. The temperature is ramped to 500^0C at a rate of 5^0C/min and held at 500^0C for 1 hour. It is then raised to 600^0C at 3^0C/min and held for another hour. After this thermal treatment, the furnace power is turned off and the sample is allowed to cool to room temperature. At this stage the developed region of the Foturan glass turns a brown color. The cooled sample is then soaked in a solution of 10% hydrofluoric (HF) acid in an ultrasonic bath for 5 min and then 12 minutes in a 5% HF bath to remove all modified volumes and then rinsed three times with DI water. Finally, the etched sample is thermally treated at 590^0C for 9 hours for further smoothing of the surface. Having completed this manufacturing procedure, the microlens array mold was imaged in an FESEM, the images are shown in Figure 2-1. The lens on the left shows all four lenses; the image on the right is a close up of the left

side of the bottom lens. The imperfections are due to the fact that the sample was not etched with HF for long enough. Figure 2-2 displays the PDMS microlens array obtained from a single lens mold which was etched for the amount of time detailed above. That mold doesn't have these imperfections because there was less lens material to remove than was the case for the four lens mold (and thus the material was completely removed before the smoothing processing at 590^0C). These imperfections in this microlens array should not greatly affect cell performance in this experiment since imaging is not required.

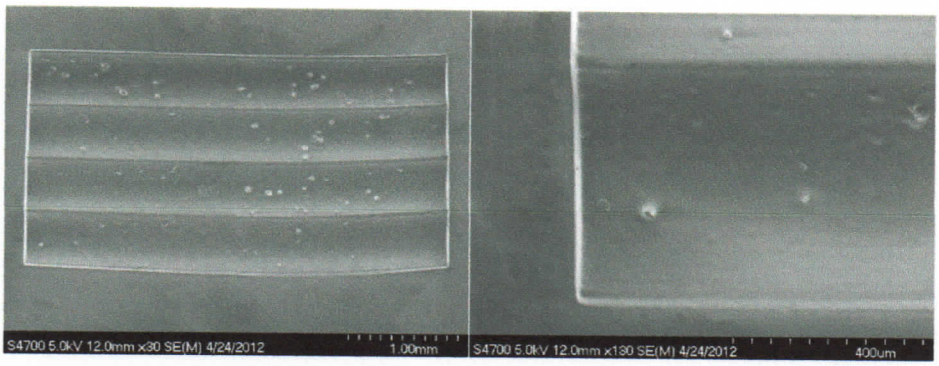

Figure 2-1. FESEM Images of Microlens Array Mold.

2.2. PDMS MICROLENS ARRAY FABRICATION

Once the mold is ready, the Polydimethylsiloxane (PDMS) lenses can be fabricated. In order to make one such lens array, begin by pouring 3mL of PDMS base into a 5mL container. Inject 0.3mL catalyst (curing agent) into the base using a pipette. Stir the solution for 1 minute. Place the glass mold in another 5mL container. Pour the stirred solution over the glass mold. Next the 5mL container containing the glass mold must be placed in a vacuum at pressure of less than 20 inch/Hg. Allow the mixture to De-gas for 1 hour. During the time spent in the vacuum chamber, the bubbles that were created in the solution during mixing will be removed. After 1 hour in the vacuum chamber, the solution should be free of bubbles. Next the mixture must be cured. This is accomplished by heating the substrate to 70^0C in a furnace for 1 hour. After 1 hour in the furnace, the PDMS should be a solid and can be removed from the mold. The mold is now ready to be used to create another PDMS lens array. The PDMS lens array is put aside until the CdTe/CdS solar cell is complete. FESEM images of a PDMS lens array created from a single-lens array mold is shown in Figure 2-2. There are very few imperfections and the lens has remarkably good smoothness, comparable to that obtained in previous research[4].

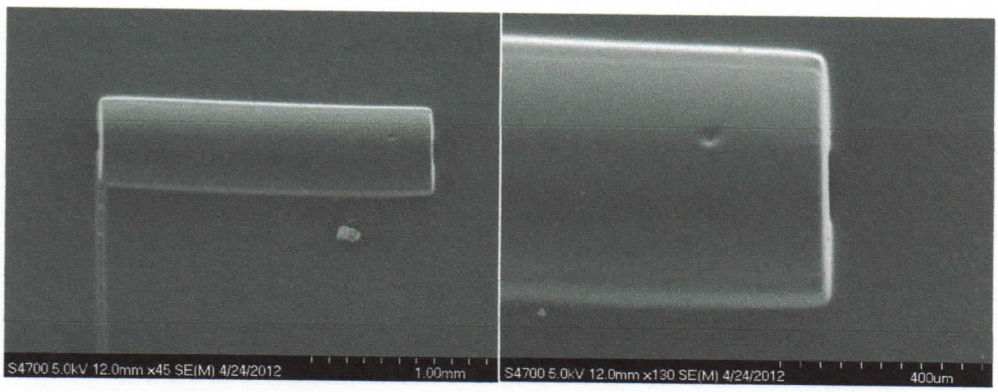

Figure 2-2. PDMS Lens Fabricated From a Single Lens Array Mold.

2.3 CdS THIN FILM FABRICATION

For the electrode on the top side of the solar cell, a thin film of SnO_2:F (Pilkington TEC-C10), a transparent conductive oxide (TCO), is used. Atop the TCO, a 150nm thick layer of CdS is deposited using a chemical deposition technique[9]. A 300mL beaker is placed on a hotplate with magnetic stirring capacity (Fischer Scientific) and filled with 250mL of distilled water. The DI water is heated to 88^0C. The TCO coated substrate is cleaned using Isopropanol then placed on the periphery of the beaker. To prevent rapid heating of water (which would disturb the samples) the setting on the hot plate should remain relatively low (setting 5 where 10 is maximum). Additionally, the stirring should be relatively gentle, so the stir setting should be the lowest available stir setting. If the heat is too high or the stir is too rough, the substrates will move around during the deposition process (they may flip over causing the film to be deposited on the side opposite of desired). When 88^0C is reached, add 6mL of a 0.033M Cadmium

Acetate (purity 99.999% Alfa Aesar) solution, 3.75mL of a 7.5M Ammonium Acetate (MP Biomedicals) solution, and 11.25mL of a 15M Ammonia solution. The Ammonia should be added slowly to prevent rapid reaction (causes non-uniformity). Wait 10 minutes. Then add 3mL of a 0.067M Thiourea (purity 99% Alfa Aesar) solution. 3mL of Thiourea will be added three more times in 10 minute intervals. After the final addition of Thiourea, wait 8 minutes before removing the substrate. When substrate is removed from the bath, place it in warm DI water and sonicate 3 times for 2 minutes each. Finally, blow the substrate dry with Nitrogen. The CdS layer should be 150nm thick after this process. CdS layer obtained was 156 ± 15nm thick. The thickness measurements for CdS were obtained using profilometry. Four measurements were taken and averaged to get the thickness (±15nm is the standard error, or twice the standard deviation divided by the square root of the number of measurements). The beakers will need to be cleaned with HCl followed by warm water. Also, HCl may be used to wipe the bottom side of the solar cell clean so that the CdS thin film remains only on the side with the TCO. The thickness of the CdS layers was determined with a profilometer using 4 different samples taking 5 measurements per sample and taking the average value. The error is determined by the standard deviation in the measurements.

After the CdS layer is deposited on the TCO, a part of it needs to be removed so that the TCO layer remains exposed (so that both contacts are available to be used in characterization). This is done by wiping away some of the CdS film on one side with HCl. This process must be carried out very carefully since even a small drop of HCl can cause significant damage to the CdS film.

2.4 CdTe LAYER FABRICATION

The process of depositing CdTe using a nanosecond laser to melt CdTe powder (purity 99.999% Alfa Aesar) as an additive manufacturing technique is reported. There are many techniques for depositing CdTe thin films including: magnetron sputtering[10], Bridgman growth method[11], electrochemical deposition[12], spray pyrolysis[13], screen-printing[5], and most popularly close-spaced sublimation (CSS) [7, 9, 14, 15, 16]. The choice of laser melting in this project was due to convenience. In order to melt CdTe powder, a melting temperature of 1092^0C needs to be reached. The melting point of Cadmium is 765^0C. So, any technique that successfully melts CdTe will vaporize some of the Cd present in the material. This causes appropriate doping of the CdTe layer for solar cell uses, but it also causes the release of Cd vapor into the laboratory environment. Laser melting provides the benefit of not releasing Cd vapor into the laboratory. Following the precedent established in the literature, a vacuum chamber was not constructed inside which to perform this laser melting[17,18]. The Cd vapor would be a major concern were it not for the melting occurring via laser material interaction. During the laser melting process the material will stay in a melted state for very small time scales. This means that very little Cd will have a chance to vaporize. Adding this to the fact that the sample sizes being used are very small, the Cd vapor doesn't pose a major health risk. Just to be on the safe side, though, a mask was worn at all times during the deposition process and the room was well ventilated. The laser system used for laser melting experiments was an Nd:YAG laser with a wavelength of 355nm and pulse duration 30ns. Samples were prepared by adding CdTe powder on top of CdS thin film and carefully leveling the CdTe powder. Samples were irradiated in air at 300K. The nanosecond laser was instructed to

pass over the length of the sample by moving 4.5mm in the y direction at a speed of 10mm/min. Then the sample was moved 0.01mm in the x direction and the laser moved back -4.5mm in the y direction. The sample is then again moved 0.01mm in the x direction. This process was repeated to cover the entire 4.5mm by 5mm surface. The laser was set to a pulse rate of 7500 Hz with a current of 46.14 A (94.5% of maximum current for our laser system) leading to a pulse energy of 105uJ at 0.80W. These laser settings are above the threshold for CdTe melting when the speed is 10mm/min. If speed of motion stage were decreased, melting would occur at a lower power. Also, CdTe melting depends on the thickness of the desired melting. With a thicker layer being melted, a higher power will be required. The thickness of the CdTe layer that resulted from the process was greater than 10 microns; the exact thickness is hard to say because profilometry is difficult with non-uniform samples. The required thickness is 2 microns to absorb sufficient amounts of incident light. The desired thickness was 5 microns to make sure none of the Cu is able to infiltrate into the CdS layer. It is difficult to control the thickness precisely using the nanosecond laser melting technique. This technique has also been used to produce a melted CdTe layer as thick as several hundred microns, albeit at much higher laser power (44.4uJ and 0.98W). It has been reported in the literature that the melting threshold for CdTe using a ruby nanosecond laser is 120mJ/cm^2 and 40mJ/cm^2 depending on the pulse duration[17,18]. The melting threshold has been determined to be approximately 27mJ/cm^2 at a laser power of 0.80W for the ns laser system. The melting threshold is lower for several reasons. First, pulse rate is higher with Nd:YAG than with ruby laser. Second, the Nd:YAG laser has a different wavelength than does a ruby laser. This method of CdTe thin film manufacture is not

cost effective for use in industry. The process requires far too much dedicated laser time (four hours to produce a 4.5 by 5mm sample) to be competitive with other available methods of manufacturing CdTe thin films. The method which seems to be the most easily scalable is the CSS method, which is commonly used. SEM images of the CdTe layer that was fabricated using my nanosecond laser melting technique is shown in Figure 2-3. Non-uniformity may infringe on cell performance. Also the porosity of the CdTe layer might allow for some level of electrical contact between the back contact and the CdS layer resulting in decreased performance.

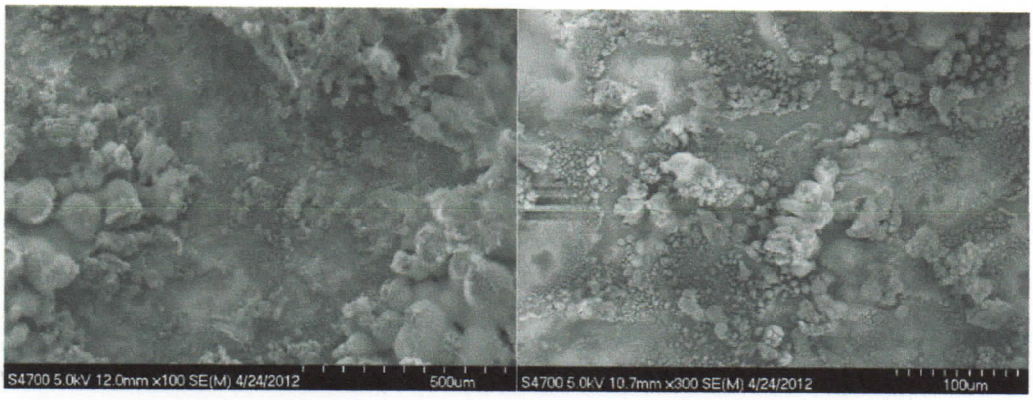

Figure 2-3. CdTe Layer SEM Images. SEM images of the surface of CdTe layer deposited by nanosecond laser melting. It can be seen that the surface is very irregular with many nanoparticles and aggregates. The image on the right is a close up of the center of the image on the left.

2.5 $CdCl_2$ THERMAL TREATMENT

CdTe and CdS form an n-p junction (n is CdS and p is CdTe). The p doping of the CdTe is due to the high temperature (>1092^{0}C) deposition which causes Cd (which has a lower melting point of 765^{0}C) to vaporize, giving rise to a Cd deficiency. CdS is chosen as a material because it is n-type doped and the transmission rate for the visible spectrum is quite good through CdS (its bandgap is 2.5eV[15]). This combined with CdTe being a great absorber of the visible part of the spectrum makes them a good choice for solar cell materials. But there is a problem: the CdS/CdTe junction has a lattice mismatch which will cause poor device performance. The solution to this problem is a $CdCl_2$ thermal treatment.

After the CdTe deposition procedure is complete, a $CdCl_2$ anneal is performed. Without the $CdCl_2$ anneal, CdTe cells generally have efficiencies between 6 and 10%, whereas cells made with the $CdCl_2$ anneal are generally more than 12% efficient[9]. Hence, the $CdCl_2$ treatment represents a crucial step in the device fabrication procedure for CdTe/CdS solar cells. $CdCl_2$ modifies the crystalline grain boundaries in the CdTe and CdS thin films[19]. It also promotes impurities in the CdTe thin film[19], further doping the CdTe. Thus, the $CdCl_2$ treatment is sometimes called thermal activation of the cell. The $CdCl_2$ treatment used in this research proceeds as follows. CdTe deposited substrates are annealed at 400^{0}C for 30 minutes in programmable furnace. A 75% saturated $CdCl_2$ (purity 99.998% Alfa Aesar) in methanol solution is prepared in a beaker on a hot plate and raised to 55^{0}C. The CdTe deposited substrates are soaked for 5 minutes in the $CdCl_2$ solution. The saturated $CdCl_2$ solution contains 1.5g $CdCl_2$ in 100mL of methanol. It is important that this soaking procedure happen under a fume

hood. $CdCl_2$ vapor is toxic if inhaled. Next the substrates are removed from the $CdCl_2$ bath and blown dry with N_2. Finally, the substrates are annealed again at 400^0C for 30 minutes in programmable furnace. The annealing procedure serves to enhance the chemical modifications made by the $CdCl_2$ interacting with the CdTe thin film[8] as well as remove $CdCl_2$ residue from the substrate surface[15]. The result of the $CdCl_2$ thermal treatment is a cell with a thin white layer of $CdCl_2$ on top the CdTe. The effect is the production of a grey look to the sample. An image of a CdTe deposited sample and a sample that was then underwent $CdCl_2$ thermal treatment is shown in Figure 2-4. The lack of uniformity obtained from the CdTe nanosecond laser melting can be seen in the image on the left. The image on the right shows that the non-uniformity problem is resolved at least partly by the $CdCl_2$ treatment.

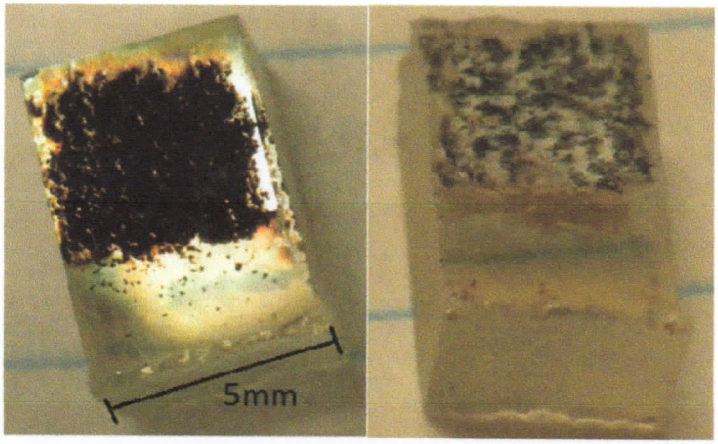

Figure 2-4. CdTe with and without $CdCl_2$. Digital camera image of CdTe deposited sample (left) and $CdCl_2$ deposited sample (right).

2.6 BACK CONTACT

The next step in the process is to deposit the back contact onto the annealed CdTe layer. The back contact is composed of 11nm of Cu and 50nm of Au. Both layers are deposited using a sputtering technique. The sputter used is a Denton Vacuum Discovery – 18 Deposition System. It allows for the operation of three sputter sources and the ability to heat, RF bias, and rotate the substrate. Thickness uniformity of films is specified as 5%. The sputtering process begins by pumping down the vacuum chamber to less than 10^{-7} Torr. Argon gas is set to flow across the sputter target. The wattage of the power source is set to 100W. The stage is set to rotate to encourage uniformity in the film. First the sputter must run with applied power for 5 minutes to clean away any contaminants, then the sputtering of the layer may commence. The deposition time for the Cu layer is 30 seconds. For the Au layer, the deposition time is 1 minute 15 seconds. The resulting thickness of the Cu layer is 10 ± 6nm. The thickness of the Au is 52 ± 10nm. Again, these thickness measurements are taken by profilometry. The large error observed in the thickness measurements for the back contact films is due in large part to the poor quality of the profilometer used in thickness measurements. Despite the poor instrument, the films lay within the desired thickness regimes. The Au in the back contact is used because of its high inherent conductivity. The Cu in the back contact can dope the CdTe surface with a p^+ region and form a back contact with lower barrier height[12]. However, Cu can also diffuse into the CdS layer causing poor device performance. This is why the CdTe layer needs to be 5 micrometers thick instead of 2 micrometers thick (the requirement for sufficient incident light absorption). The thicker CdTe layer reduces the chance of Cu diffusing into the CdS layer. The back contact

deposition of samples that underwent electrical characterization was performed by Dr. Kevin Leedy of the Air Force Research Lab at Wright Patterson Air Force Base due to technical difficulties with the sputtering machine on MS&T campus.

2.7 COMPLETED DESIGN

Having completed the Cu/Au back contact, the solar cell is complete. The solar cell is a six layer solar cell design: float glass/SnO_2:F/CdS/CdTe/Cu/Au. On top the float glass the microlens array will be added to complete the design. The way the PDMS lens array is added is relatively simple. The solar cell is heated to 100^0C. Once it reaches 100^0C, the PDMS lens array is placed on top. The solar cell with PDMS layer on top is allowed to cool to room temperature. When it has cooled, the PDMS layer is adhered to the float glass. The lens array is not damaged in this adhesion process. Thus, the end resulting design will be PDMS/Float glass/SnO_2:F/CdS/CdTe/Cu/Au. Final solar cell design is shown in Figure 2-5. Staggering of layers, shown in Figure 2-5, is required for several reasons. First, contact between back contact and the TCO will result in a short in the system which will severely inhibit performance. Second, Cu cannot diffuse into the CdS layer without harming performance. Staggering of each layer helps to prevent electrical contact between back contact and TCO while also reducing the chance that Cu will diffuse into the CdS layer.

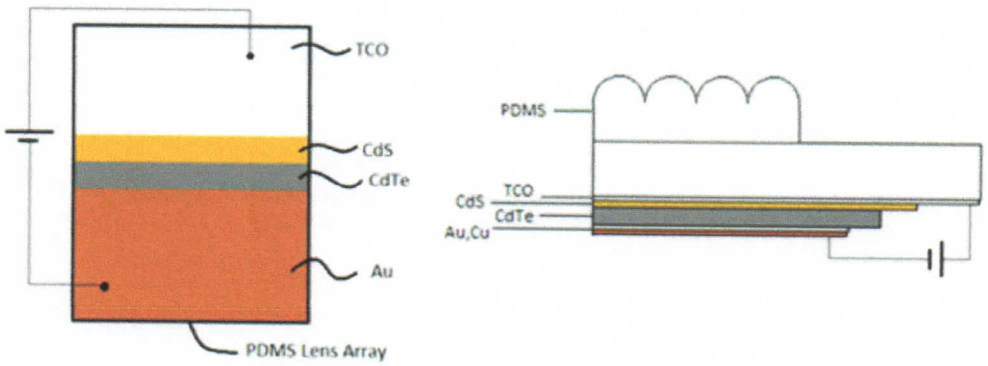

Figure 2-5. Completed Cell Design. A top view of the cell design (left) shows the staggering of the CdS, CdTe, Au layers required to obtain optimal performance. A side view of the cell (right) shows the relative thickness of the films. Electrical measurements were made between the Au and TCO layers across the maximum length of the solar cell.

3. RESULTS AND ANALYSIS

3.1 SOLAR CELL CHARACTERIZATION

A 3300K Halogen high intensity illuminator (Edmund Optics, MI 150) was used to approximate incident sunlight for solar cell characterization. Better approximations of sunlight can come from Metal Halide arc lamps or solar simulators, such as those available through Newport. The value of using these devices is that they better approximate the radiation spectrum of the sun. Thus, they will give more accurate estimates of efficiency. But, using a Halogen illuminator will give a good idea of the efficiency of this cell design.

A MyDAQ data acquisition unit from National Instruments was used with a simple Labview program as a voltage source. Voltage was applied from -1V to +1V between the TCO and the gold layer of the back contact. Two multimeters, each with μA and mV resolution, were used to verify the voltage being applied and to record the current flowing between the TCO and back contact at each voltage value (in 0.2V steps). This process was applied to the solar cell first in the dark (with no incident light) and then with the high intensity illuminator. Data was collected at each voltage value by averaging over four data points. Three sets of data, each with four samples, were collected for comparison. The first was for solar cells constructed without the $CdCl_2$ thermal treatment and without a microlens array. The second was with $CdCl_2$ treatment and without a microlens array. The third was with $CdCl_2$ treatment and the microlens array. This was done so that the cell performance with and without $CdCl_2$ might be determined as well as the effect of the microlens array.

3.2 CURRENT AND VOLTAGE CHARACTERISTICS

The solar cells constructed without the $CdCl_2$ treatment proved difficult when it came to electrical characterization. The leak current in the cell varied considerably between cells. An example of the behavior displayed by the cells without $CdCl_2$ treatment can be seen in Table 3-1. From the table it is obvious that the cell performance without light (dark current) deviates significantly between the two cells. The current obtained without light is called dark current and represents the current that leaks across the cell (thus it is called leak current). This current is not useful to be applied to the load. The fact that the leak current differs significantly between cells means that the quality and uniformity differ significantly between cells. This could be due to the properties of the CdTe layer. From SEM images in Figure 2-3, it can be determined that many nanostructures are present in the CdTe layer and that the layer itself is highly non-uniform.

The lack of uniformity of the CdTe layer means that it is very porous. This porosity may have allowed the back contact to come into direct electrical contact with the CdS layer; which would cause much higher leak currents. Another source of problems could have been in the laser melting of CdTe. The laser melting process did not vaporize Cd from the CdTe; this may have insufficiently doped the semiconducting layer. This insufficient doping may have hampered cell performance. Additionally, Cu may have diffused into the CdS layer hampering cell performance. The data certainly confirms high variations in leak current.

Table 3-1. Electrical Characterization of Cells without $CdCl_2$.

Voltage (V)	Sample 1, Dark Current (mA)	Sample 1, Light Current (mA)	Sample 2, Dark Current (mA)	Sample 2, Light Current (mA)
1	1.4385	1.991	0.283	0.348
0.8	1.0535	1.453	0.213	0.25
0.6	0.731	1.107	0.145	0.169
0.4	0.4125	0.727	0.09	0.106
0.2	0.1775	0.366	0.043	0.047
0	0.003	0.003	0.002	0.003
-0.2	-0.2075	-0.388	-0.039	-0.039
-0.4	-0.4415	-0.822	-0.082	-0.082
-0.6	-0.7095	-1.246	-0.128	-0.253
-0.8	-0.9675	-1.755	-0.178	-0.361
-1	-1.2715	-2.206	-0.234	-0.494

The solar cells which underwent $CdCl_2$ treatment before sputtering of the back contact displayed much more reliable responses in the characterization process. The values obtained for leak currents were very comparable and so was the response under high intensity illumination. This higher level of reliability (and overall lower leak currents) may be, in part, due to the fact that the $CdCl_2$ increased uniformity of the surface by filling in the low lying areas (as seen in Figure 2-4). The increased performance is likely due to the fact that the $CdCl_2$ treatment has been shown in many experiments to increase efficiency as much as twofold as discussed in Section 2.5. Additional comparison of uniformity can be made by use of Figure 3-1. Performance of $CdCl_2$ treated cells is compared with untreated cells in Figure 3-2 and Figure 3-3.

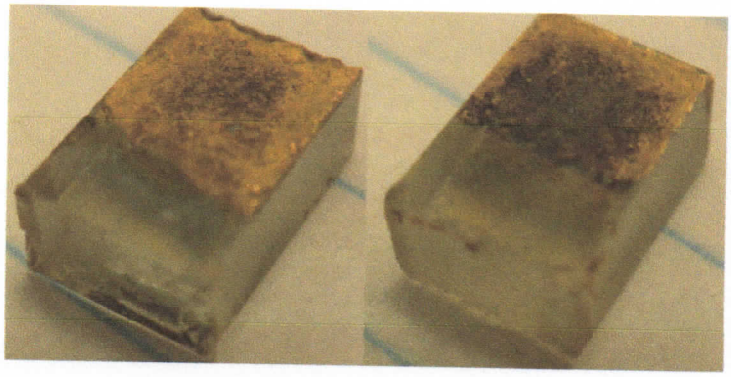

Figure 3-1. Treated (left) and Untreated (right) Cells after Sputtering of Back Contact.

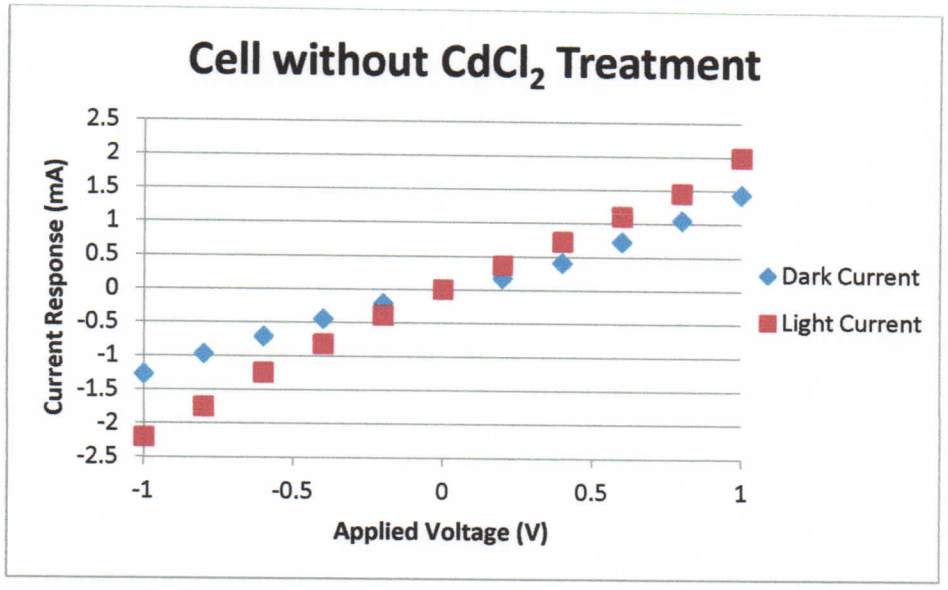

Figure 3-2. Electrical Characterization of Cell without $CdCl_2$ Thermal Treatment.

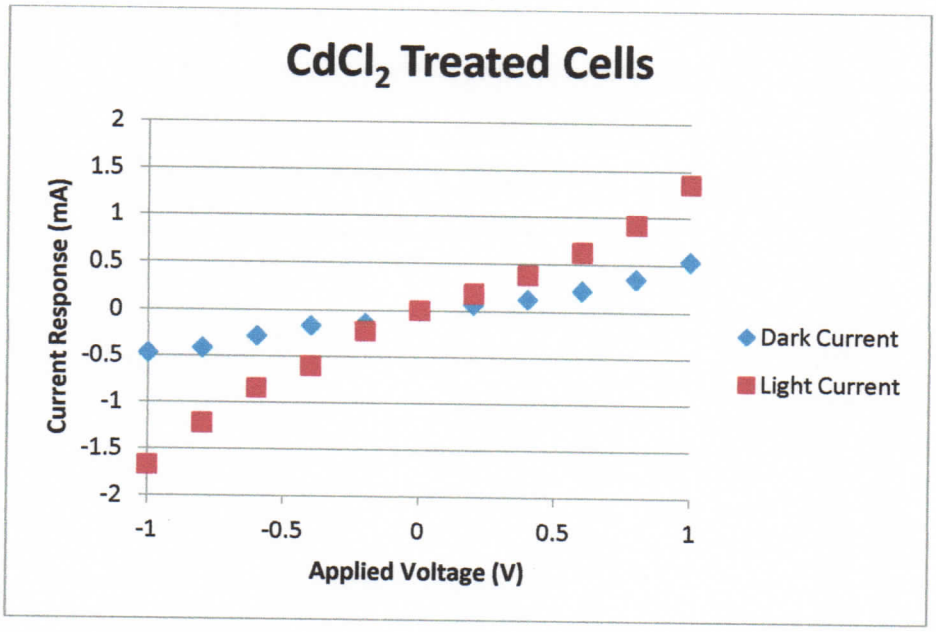

Figure 3-3. Electrical Characterization of $CdCl_2$ Treated Cells.

The $CdCl_2$ treated samples which were characterized to produce Figure 3-2 were then characterized again after having the PDMS lens array added to them. This procedure turned out to be unexpectedly problematic. The cells seem to have been damaged when having undergone high voltages for long timescales when being characterized without microlens arrays. Table 3-2 displays the average values recorded for one sample. Take note of the very high values of standard deviation in the far right column. The values in this table represent the average over 15 measurements at each voltage value. It took 15 measurements to obtain an average value that did not significantly change when a new value was added to it. Additionally, the values for each sample differed greatly, with two of the samples exhibiting electrical shorts before data could be completed (these two were not included in the data set). Another possible source of this variability could be the apparatus. The electrical measurement system

consisted of two wires pressing down on either side of the cell surface to make good electrical contact. These wires could move a small amount during the process and occasionally did so; this could have caused mechanical damage to the surface of the cell allowing for electrical shorting in later measurements.

Keeping these difficulties in mind, the results that were obtained may not be highly accurate. The results from the microlens array enhanced cells are displayed in Figure 3-4. The results seem to indicate a much higher level of performance when the microlens array is used. Assuming these results are accurate (considering the difficulties encountered), they confirm the proposed theory. The performance of the cells with the microlens array added shows a comparable absolute value of increase in current with incident light than does the cells without the microlens array. However, the leak current is much lower with the microlens array data, so the percentage difference is much higher with the microlens arrays than without. This seems to indicate that the microlens array enhances the cell performance.

Table 3-2. Electrical Characterization of Cells with Microlens Arrays.

Voltage (V)	Dark Current Average (mA)	Light Current Average (mA)	Dark Current Standard Deviation (mA)	Light Current Standard Deviation (mA)
1	0.147	0.852	0.040	0.413
0.8	0.113	0.739	0.043	0.334
0.6	0.091	0.548	0.052	0.147
0.4	0.057	0.335	0.029	0.099
0.2	0.017	0.215	0.003	0.045
0	0.004	0.004	0.000	0.000
-0.2	0.052	0.214	0.054	0.103
-0.4	0.031	0.443	0.019	0.191
-0.6	0.069	0.723	0.053	0.257
-0.8	0.137	1.047	0.133	0.372
-1	1.755	1.701	0.631	0.530

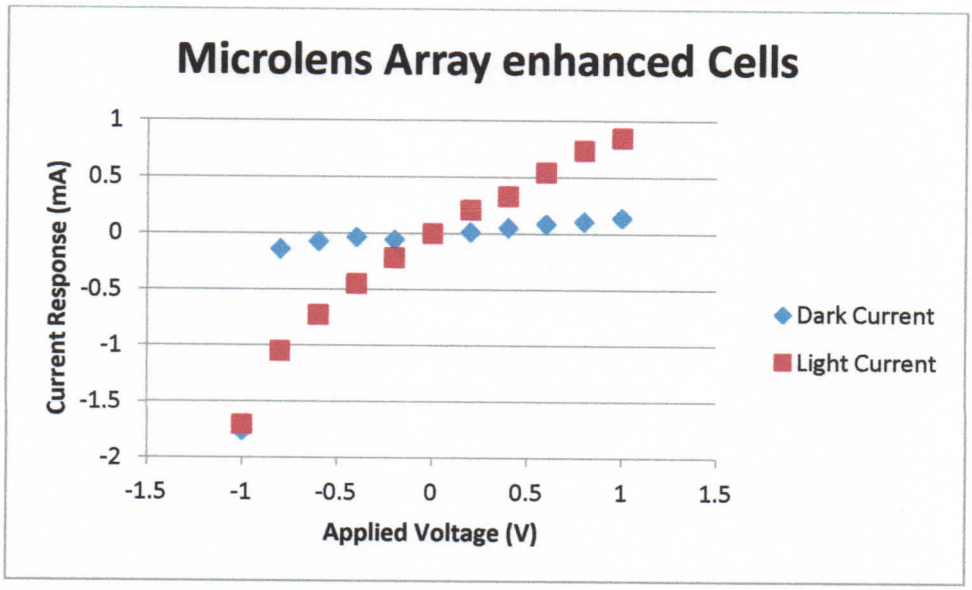

Figure 3-4. Characterization of Microlens Array Enhanced Cells.

3.3 DISCUSSION

The primary indicator for solar cell performance in industry is the efficiency of energy conversion. Efficiencies for typical CdTe/CdS solar cells, as mentioned in the introduction, are approximately 12%. The efficiency is calculated from the following equation.

$$\eta = \frac{P_{electric}}{I * A_C}$$

Where I is the intensity, A_C is the cell area, and $P_{electric}$ is the usable electric power output of the cell. The usable power output of this cell (power with high intensity light minus power lost due to leak current) is on the order of 1mW. The intensity, calculated based on parameters of the light source, is 1,738.94 W/m^2. Then the efficiency of the cell without the microlens array is 2.19%; with the lens array it is 2.26%. Thus the overall efficiency of the cells is very small, but a notable improvement is seen with the lens array in place. The small efficiencies observed are likely due to the CdTe layer fabrication. The TCO, CdS, Cu, and Au layers are not likely candidates for problems. They proved highly uniform and their manufacturing techniques were reliable. The $CdCl_2$ procedure was only carried out once, but it was a straightforward procedure following that which was done in the literature. Additionally, the $CdCl_2$ treated cells performed much better than their counterparts without the $CdCl_2$ treatment. The only remaining layer that could be at fault was the CdTe layer. This layer was fabricated using a laser melting technique. As discussed in Section 2.4, this layer is known to exhibit high levels of non-uniformity as well as the presence of unwanted nanostructures. This non-uniformity may very well be the source of the unreliability in data collection, allowing for high leak current and interaction between Cu and CdS layer. Another possible performance reduction could

come from the fact that laser melting avoids Cd vaporization. As mentioned in Section 2.4, this vaporization of Cd, while toxic, serves to appropriately dope the CdTe layer. The fact that this doping didn't take place in the laser melting procedure could prove to be the source of the low efficiency that is observed.

BIBLIOGRAPHY

1. Kamat, Prashant V. (2007) **Meeting the Clean Energy Demand: Nanostructure Architectures for Solar Energy Conversion.** *J. Phys. Chem.* 111: 2834 – 2860.

2. A. Luque. (2011) **Will we exceed 50% efficiency in photovoltaics?** *Journal of Applied Physics.* 110: 031301

3. Yang J, Banerjee A, Glatfelter T, Hoffman K, Xu X, Guha S. (1994) **Progress in triple-junction amorphous silicon-based alloy solar cells and modules using hydrogen dilution**. *Proceedings of the 1st World Conference on Photovoltaic Energy Conversion.* 380–385.

4. C. H. Lin, L. Jiang, Y. H. Chai, H. Xiao, S. J. Chen, H. L. Tsai. (2009) **Fabrication of mircolens arrays in photosensitive glass by femtosecond laser direct writing.** *Applied Physics A.* 97: 751 – 757.

5. K.L. Chopra, P.D. Paulson, and V. Dutta. (2004) **Thin-Film Solar Cells: An Overview**. *Progress in photovoltiacs: research and applications.* 12: 69-92.

6. Duffie, John A. and William A. Beckman, Solar Engineering of Thermal Processes. New Jersey: John Wiley & Sons, Inc, 2006.

7. Wu, Xuanzhi. (2004) **High-efficiency polycrystalline CdTe thin-film solar cells**. *Solar Energy.* 77: 803 – 814.

8. J. R. Tuttle, M. A. Contreras, T. J. Gillespie, K. R. Ramanathan, A. L. Tennant, J. Keane, A. M. Gabor, R. Noufi. (1995) **Accelerated publication 17.1% efficient Cu(In, Ga)Se_2 – based thin-film solar cell.** *Progress in Photovoltaics: Research and Applications,* 3:235-238.

9. Rose, D. H., F. S. Hasoon, R. G. Dhere, D. S. Albin, R. M. Ribelin, X. S. Li, Y. Mahathongdy, T. A. Gessert, and P. Sheldon. (1999) **Fabrication Procedures and Process Sensitivies for CdS/CdTe Solar Cells.** *Progress in Photovoltaics: Research and Applications.* 7: 331 – 340.

10. Compaan, A. D., A. Gupta, S. Lee, S. Wang, and J. Drayton. (2004) **High efficiency magnetron sputtered CdS/CdTe solar cells.** *Solar Energy.* 77: 815 – 822.

11. E. Saucedo, P. Rudolph, E. Dieguez. (2007) **Modified Bridgman growth of CdTe crystals.** *Journal of Crystal Growth.* 310: 2067-2071.

12. A. C. Rastogi, R. K. Sharma. (2009) **Properties and mechanism of solar absorber CdTe thin film synthesis by unipolar galvanic pulsed electrodeposition.** *J. Appl. Electrochem.* 39: 167-176.

13. J. L. Boone, T. P. Van Doren, A. K. Berry. (1982) **Deposition of CdTe by Spray Pyrolysis.** *Thin Solid Films.* 87: 259-264.

14. I. Polat, S. Yilmaz, E. Bacaksiz, M. Altunbas, and M. Tomakin. (2011) **Effect of $CdCl_2$ annealing on the crystalline transformation of CdTe thin films grown by evaporation at a low substrate temperature.** *Turk J. Phys.* 35: 197 – 202.

15. D. Bonnet. **Manufacturing of CSS CdTe solar cells**. (2000) *Thin solid films.* 361-362; 547-552.

16. X. Wu, J. Zhou, A. Duda, Y. Yan, G. Teeter, S. Asher, W. K. Metzger, S. Demtsu, S. Wei, R. Noufi. (2007) **Phase control of Cu_xTe film and its effects on CdS/CdTe solar cells**. *Thin solid films.* 515; 5798-5803.

17. L. A. Golovan, P. K. Kashkarov, and V. Y. Timoshenko. (1996) **Laser-Induced Melting and Defect Formation in Cadmium Telluride**. *Interation of Laser Radiation with Matter.* 6: 925 – 927.

18. E. Gatskevich, G. Ivlev, P. Prikryl, R. Cerny, V. Chab, O. Cibulka. (2005) **Pulsed laser-induced phase transformations in CdTe single crystals.** *Applied surface science.* 248: 259-263.

19. M. Emziane, C. J. Ottley, K. Durose, and D. P. Halliday. (2004) **Impurity analysis of $CdCl_2$ used for thermal activation of CdTe-based solar cells.** *Journal of Physics D: Applied Physics.* 37: 2962 – 2965.

VITA

Patrick M. Margavio was born in Tuscaloosa, Alabama. In May 2010, he received his B.S. with Honors in Physics and Applied Mathematics from Missouri State University in Springfield, Missouri. He was voted Outstanding Undergraduate Student by MSU Physics Faculty in 2007. He was inducted into Phi Kappa Phi National Honors Society in 2007. He won first place in a Missouri Academy of Science presentation in 2009. In August 2012, he received his M.S. in Mechanical Engineering from Missouri University of Science and Technology.